(ANSR Rpt. SL_Ex1)

Hydrodynamic Simulations for a Prototypical Sonoluminescent Air-Bubble-in-Water Example

William C. Mead

(wcm@ansr.com)

Adaptive Network Solutions Research, Inc., Los Alamos, NM

Report prepared for Impulse Devices, Inc.

Grass Valley, CA

August 28, 2000

Copyright 2000 by Adaptive Network Solutions Research, Inc. and Impulse Devices, Inc.

ANSR is a trademark of Adaptive Network Solutions Research, Inc.

Contents

I. Introduction and Background

Overview

This report discusses the results of calculations of several hydrodynamic test cases and a particular sonoluminescent (SL) bubble example,[1,2] using the computer hydrodynamics code HYADES.[3,4] Our goal in this work has been primarily to build a foundation for subsequent work that will study bubble dynamics in conceptual designs for investigating Sonically Driven Fusion (also referred to as Sonic Fusion or simply SF) reactor scenarios. Our subsidiary goal has been to learn as much as we can about SL physics and dynamics from the extensive previous work in the field, and especially from the early simulation work of Moss, et al.[2] At the outset, we should point out that Moss has revisited SL simulations subsequently using more elaborate physical modeling in order to obtain detailed predictions of the SL radiation spectrum and timing.[5,6] In the work reported here, our modeling has been limited in physics scope to correspond with that of Moss, et al.'s 1994 work, neglecting thermal conduction and radiation.

In Section I of this report, we present background material on HYADES' physical models. We list some known omissions from the HYADES modeling and discuss the potential impact on SL modeling. We then briefly recap results from hydrodynamic test calculations that allow us to examine HYADES' modeling performance in the light of relevant cases with known analytic solutions.

In Sec. II, we present the initial conditions for the SL example we will be discussing throughout this work. We discuss our first HYADES results for the prototype SL example. We discuss the main physical processes that lead to concentration of a portion of the acoustic driving energy into a tiny, hot, dense collapsed core that emits a pulse of light.

Section III presents results from a more detailed examination of the SL example. We present some important numerical and diagnostic techniques. We discuss the simulation issues of numerical accuracy, speed, and convergence as they apply to the SL calculations. Next, we discuss the calculated physical conditions around the time of bubble collapse (near stagnation). We compare our results in some detail with the previous work[2] of Moss, Clarke, White, and Young. We compare some of the salient features of our simulations with the current body of SL measurements to determine the extent to which our calculations offer a reasonable account of the processes involved.

Finally, we summarize our work and present our conclusions to date. In several broad respects, our calculations support the findings of Moss's work. We find the comparisons with experiment to be limited by several factors, but generally encouraging. We believe we have obtained a solid foundation for performing calculations to begin to assess Sonically Driven Fusion (SF) reactor scenarios, including

- a good understanding of some of the key SL physical processes,
- a set of numerical techniques that provide a reasonable level of confidence and adequate accuracy in HYADES calculations in this physical regime, and
- adequate simulation capabilities to make our theoretical explorations of the potential for SF informative and worthwhile.

HYADES Physical Models

For readers unfamiliar with the HYADES computer hydrodynamics code, we summarize in this section its physical models and its prior applications. The code has been developed by Dr. Jon T. Larsen over the past several years to help with the planning, design, and interpretation of experiments in the field of Inertial Confinement Fusion (ICF).

HYADES, in the form we have used it, is an explicit 1-Dimensional Lagrangian hydrodynamics code.[3,4] Matter is represented in 1-D planar, cylindrical, or (in most of this work) spherical cells, using tabular Equations of State (EOS). The EOS used for air was from the SESAME EOS Library.[7] For water, the EOS used was based on steam tables of the National Bureau of Standards.[8,9] HYADES' hydrodynamics model is a traditional Lagrangian finite difference formulation with a von Neumann artificial viscosity to treat shock wave formation and propagation. A linear artificial viscosity is included to dampen numerical noise and smooth the solutions slightly. The simulation time step is limited by the Courant stability condition, namely, that the time step must be less than the time required for a sound wave to cross a zone.[10] Other timestep controls are based on the rates of change of zonal volumes and temperatures.

In addition to 1-D hydrodynamics, HYADES optionally includes models of ionization, electron- and ion-thermal conduction, radiation (including both LTE and non-LTE models with single- or multigroup-diffusion), and laser light propagation and absorption.

For the present work, we have limited the physics included in the simulations to a small, key set of physics approximations as did Moss, et al. in their earliest work. Thus, for the work reported here, the calculations include only hydrodynamics modeling, using fairly realistic tabular equations of state with artificial viscosities.

Omitted Physics

It's worthwhile to list the physical processes that might play some role in bubble dynamics and that are omitted in the modeling discussed here:

- mass diffusion between the bubble gas and the surrounding liquid
- surface tension
- non-spherical geometric effects (2-D and 3-D asymmetries)
- hydrodynamic instabilities
- electron conduction
- radiation

We can argue from estimates, or from the previous work of others, that certain of these effects will not make significant changes to the bubble dynamics. For example, over most of the bubble's interface history, surface tension is much too small to alter the bubble dynamics; at most, we expect only a minor effect on the bubble dynamics. Also, at these low temperatures, radiation is unlikely to play a significant role in determining the energy balance in the bubble or water. Electron conduction cooling of the bubble could be significant, but only near the end of the implosion. Others of these effects are harder to argue into insignificance, so we incur some risk of making our calculations in an artificial universe that doesn't resemble our own. What we lose in realism, we gain in simplicity and ease of understanding—a useful benefit at this stage of the research.

HYADES Calculations of Some Relevant Hydrodynamic Test Problems

As a foundation for the work reported here, we performed a number of test calculations using HYADES to gain familiarity with the code, and to determine the performance characteristics and general accuracy of HYADES' hydrodynamics algorithms. The results of these test problem calculations have been analyzed to help establish our own views of HYADES' adequacy for undertaking the study of Sonoluminescence (SL) and Sonically Driven Fusion (SF). In this section, we'll discuss the test problems and HYADES' performance in simulating them.

Isentropic Planar Expansion of a Hot Foil

This problem begins with a 200-μm thick planar foil of "ideal-CH" (represented by an ideal gas EOS with $\gamma = 5/3$) at 1.05 g/cc density and 1 keV temperature. Here's a checklist of the features of the solution, with the accuracies of HYADES' simulation results using 128 uniformly distributed zones indicated in parentheses. The foil expands freely into a vacuum on both sides of its centerline. A rarefaction wave moves into the dense material at the sound speed (< 2%). The expansion reaches an asymptotic velocity of about 3 times the sound speed (11%). Matter remains isentropic during the expansion (5%). The expansion is symmetric about the foil's midplane (to ~1 part in 10^6).

Figure 1 shows density histories for all 128 zones in the simulation. As time increases, we see zones rarefying at successively greater depth in the foil. At t = 0.25 ns, as expected, the rarefaction reaches the center of the foil, and the entire gas then continues to decompress at densities below the initial 1.05 g/cc.

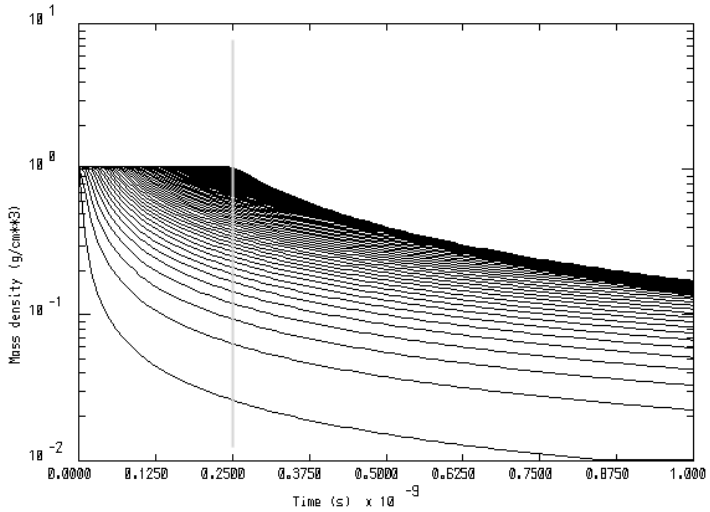

Figure 1. History of the mass density of every zone in the planar expansion test problem shows the successive density decreases as the rarefaction wave develops. The gray solid line shows the time the rarefaction is expected to reach the center of the foil. HYADES reproduces expected features of the expansion quite well.

Planar Isentropic Compression of a Warm Foil

Here, we start with a 1000-μm thick planar foil of ideal-gas (He) at 0.2 g/cc and 0.1 keV, with 50 uniform zones. The left-hand boundary of the foil is held fixed at x = 0. A piston moves inward from the right boundary at a speed that is small (1 cm/μs) compared with the sound speed in the foil (11. cm/μs). The foil is compressed isentropically with γ = 5/3 (pressure within 5% of isentropic path) to a final density of more than 100. g/cc. No significant shock waves are generated.

Figure 2 shows an "isentrope" for a single zone in the foil. By plotting log[P(t)] vs. log[ρ(t)] , we arrange for an ideal gas isentrope (line of constant entropy, $p\rho^{-\gamma}$ = const.) to be displayed as a straight line with slope γ. Evidently, HYADES calculates the isentropic compression of a γ = 5/3 ideal gas very well.

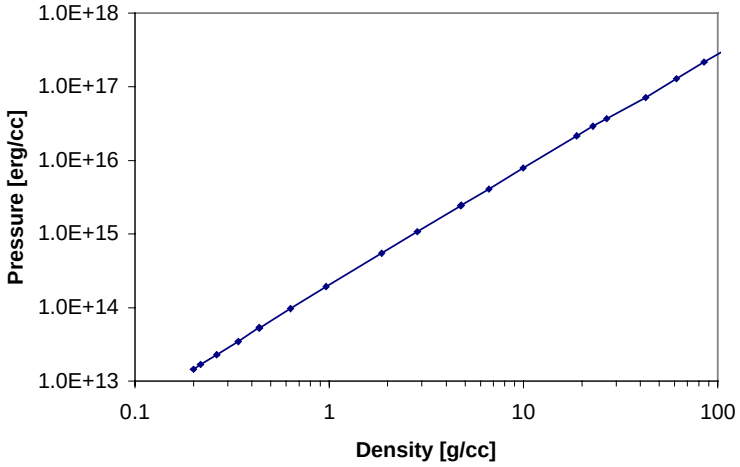

Figure 2. Isentrope of a single zone in the planar isentropic compression test case. Using an ideal gas equation of state, HYADES (dots) matches the expected isentrope (solid line) for γ = 5/3 to better than 5%.

The "Noh" Problem

In the Noh problem,[11,12] a spherical, cold ideal gas is initialized with a uniform, radially inward speed of 1 x 10^8 cm/s (except at the center). A shock forms at the origin and propagates outward as the gas stagnates. For an initial gas density of 1 g/cc, the analytic solution for γ = 5/3 predicts a density in the stagnated gas, after passage of the outward shock, of 64 g/cc. HYADES, like most other hydrodynamics codes, produces anomalous "wall-heating" near the origin. This heating causes premature stagnation, with densities much lower than predicted in the centermost cells. In a HYADES calculation using a total of 250 zones, the central 30 zones have stagnation density below 40 g/cc. Further out, and later in time, matter stagnates at densities of 50-58 g/cc. HYADES' performance, in this case, is far from ideal, as shown in Fig. 3. The extent to which the anomalous heating occurs depends on the discontinuity at the origin, so the wall heating can be considerably less than this (sometimes completely negligible) in realistic problems. If the bubble calculation does not produce a 1-zone discontinuity in velocity at the origin (as occurs in the setup of the Noh test problem), HYADES' performance might be adequate for the present application. This is potentially the most

a)

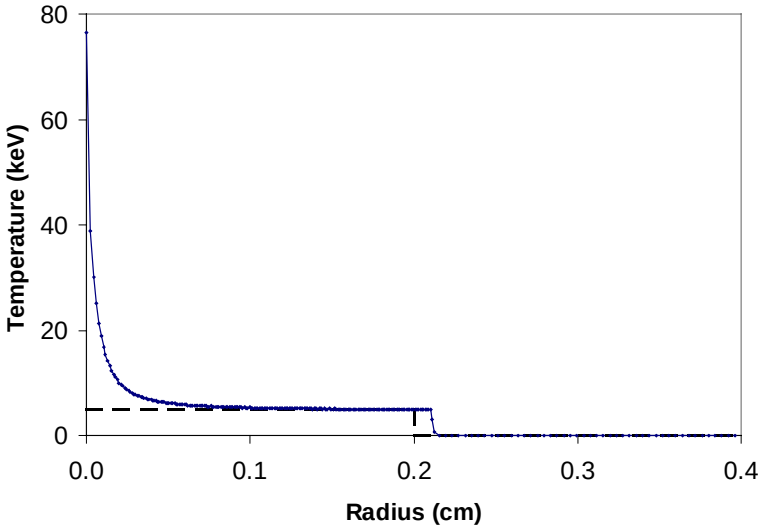

b)

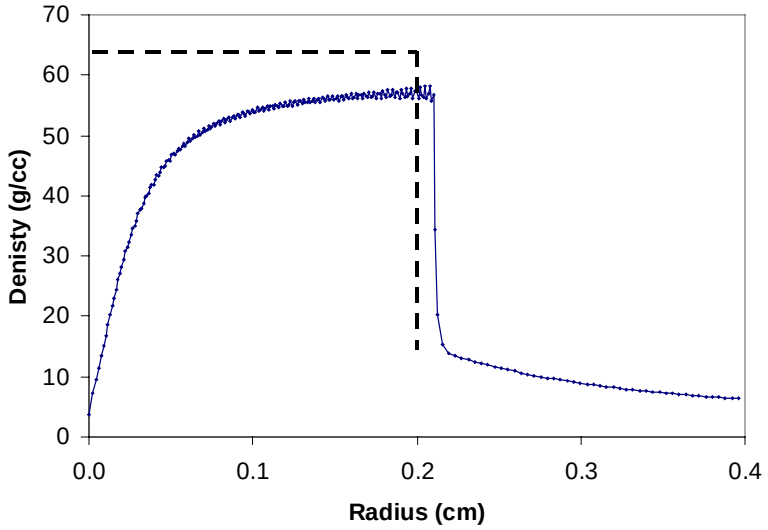

Figure 3. Noh problem (a) temperature and (b) density as calculated by HYADES (smooth curve with dot plotted for each zone-center value) and expected from analytic solution (dashed lines). Like many hydrodynamics codes, HYADES generates spurious heating in the zones near the singularity at the origin.

significant numerical difficulty we have identified in HYADES' hydrodynamics, and some special effort is required to assess the extent to which anomalous wall heating occurs in realistic SL and SF simulations.

The "Guderley" Problem

The Guderley problem [ref. 13, pp. 794-806] is related to the Noh problem, except in this case, a spherically inward-propagating shock wave is launched in a stationary medium by a piston at the outside boundary of the sphere. The shock propagates to the origin, reflects, and propagates back outward, shock-compressing the matter a second time. Here, too, a similarity solution provides detailed expectations for the shock pressure, velocity, and density as the system evolves. HYADES simulation of this test case is excellent, and a time history of the density of all zones in the calculation (Fig. 4) shows several expected features. The similarity solution predicts that the initial shock radius scales with $R \sim |t|^{\alpha}$, and Stanyukovich's numerical solution for $\gamma = 7/5$ obtained $\alpha = 0.717$ [ref. 13, p. 803]. Using HYADES with 250 zones, we obtain $\alpha = 0.75 \pm 0.03$ from the data plotted in Fig. 5. After inward passage of the direct shock, the material density is predicted to be 0.6 g/cc, and HYADES' obtains this result to better than 3% accuracy. The material density after passage of the shock reflected from the origin is predicted to be 137.5 times the initial density; HYADES calculates this density to better than 10% accuracy. Thus, HYADES' performance on this test problem is exemplary.

Inward-Moving Spherical Shock Wave in Air

This problem is a spherically converging shock, launched via an inward-moving piston, as in the Guderley problem. We use an ideal-gas EOS for air ($\gamma = 7/5$). The piston speed is much lower (5×10^3 cm/s), yielding a weaker shock with physical conditions that are close to SL values. The initial shock pressure for an initial density of 5.935×10^{-4} g/cc is 1.2 bar, consistent with an analytic estimate. With 100 zones, we calculate a maximum pressure of about 30 bar when the shock converges to the center.

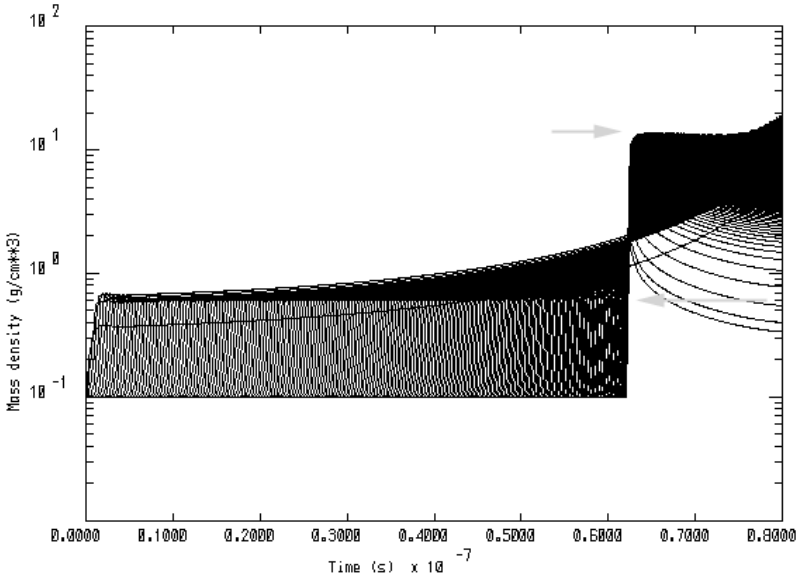

Figure 4. Density history for all zones in the HYADES simulation of the Guderley problem with $\gamma = 7/5$. Gray arrows show the expected densities after passage of the incoming and reflected shock waves. HYADES handles this test problem very well.

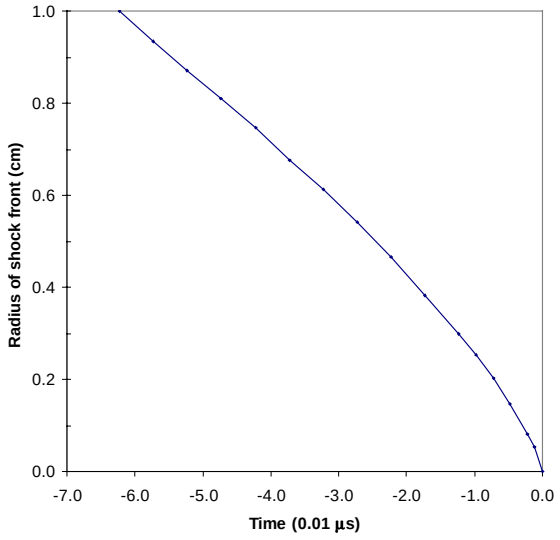

Figure 5. Radius history of the inward-moving shock front in the Guderley simulation. Plotted points were extracted by hand from the HYADES simulation at selected times. The abscissa is the time before the shock reaches the origin (as used in the similarity solution), in units of 0.01 μs. From this curve, we extract the similarity solution's parameter, $\alpha = 0.75 \pm 0.03$, in reasonable agreement with the results of Stanyukovich's numerical solution [ref. 13, p. 803].

II. The Sonoluminescent Bubble Example: A First Look

Initial Conditions

Reference 2 presents Moss, et al.'s early results for a purely hydrodynamic simulation of a generic SL bubble collapse. Moss chose an initial bubble radius of 10 μm and a water surround of radius 5 cm. The initial temperature was apparently near room temperature (we used 0.15 C for the calculations, here).[14] The initial gas density in the bubble (1.31×10^{-3} g/cc) and the initial water density were chosen so the initial pressure was 1.00 bar. Moss, et al. chose a driving pressure pulse of $P_a = 0.25$ bar peak amplitude with a sinusoidal time dependence at a frequency f = 45 kHz, i.e., $P = P_0 + P_a \sin(\omega t + \phi_0)$, with $\omega = 2\pi f$ and $\phi_0 = \pi$. Thus, the drive pulse starts at ambient pressure and decreases for the first quarter cycle. For this off-resonance choice of water surround size and driving frequency, no signal reaches the bubble until the outer drive has advanced well into its second cycle.

Dynamics of Air Bubble in Water

Moss, et al.'s calculated bubble radius history[2] is shown in Figure 6. The plot also shows the interface velocity (dotted line), and the retarded driving pressure (dashed line). The first rarefaction wave from the drive pulse reaches the bubble wall at about 33 μs. The bubble expands until the increasing drive pressure eventually causes the surrounding material to move inward. The size of the bubble has been chosen so that the timescale of the bubble expansion and initial contraction occur over about ½ cycle of the driving pressure, so the pressure difference between the water and the bubble gas is nearly maximized over a significant part of the collapse. During the early implosion phase, the pressure difference causes the water to accelerate inward. As the collapsing bubble radius decreases, spherical convergence leads to acceleration of the water next to the bubble wall. As the bubble radius shrinks, the pressure inside the bubble finally rises dramatically, the gas eventually reverses the inward motion of the wall (neglecting Rayleigh-Taylor instabilities), and the bubble again expands. In Moss's calculation, the bubble reexpansion and recollapse is rapid enough that the bubble wall undergoes a couple of minor (small, fast) oscillation cycles, before the next drive rarefaction (presumably) leads to a major expansion-collapse cycle similar to the first one.

We should point out, here, that some aspects of Moss, et al.'s calculational approach might lead to driving conditions that are different from those in experiments. The potentially different effects arising from steady state (experiment) vs. single-pulse (calculation) drive must be considered. The SL experiments drive the water and bubble repetitively, and some aspects of the dynamics might be affected by cycle-to-cycle carry-over in physical conditions. For example, if the experiment has a vessel Q >> 1, the sound field will build up over many drive cycles, and the radial pressure distribution will be different in detail from that obtained in a single-pulse calculation. We have briefly explored this effect, and our initial findings indicate that the difference between single-pulse and multi-pulse drive is not likely to affect bubble dynamics at the level of precision we are able to make comparisons. However, the overall question of the effect of repetitive vs. single-pulse drive is not fully addressed, to date. Another example of potential cycle-to-cycle physical interactions is variation in the composition of gas in the

"air" bubble. Experimentalists have obtained some evidence that the composition of the air bubble changes through repeated diffusion and heating cycles, leading to a bubble that is depleted in oxygen and nitrogen, and relatively enriched in argon content. For now, we shall neglect all these potential complications and examine the idealized single-cycle, pure-air-bubble case, as did Moss, et al.

Preliminary results of the first HYADES simulation of this SL example were presented at the IDI consultant's meeting of March 3, 2000. Figure 7 shows the bubble wall radius history from the first HYADES calculation. Qualitatively, the result corresponds quite well with Moss' calculation. Note that this plot does not resolve the rapid changes near the bubble's collapse, which occur on a short timescale compared with the plotting frequency. We'll address this issue shortly. Here, we observe that the general correspondence between the HYADES calculation and that of Moss, et al. is encouraging, at both a qualitative and semi-quantitative level.

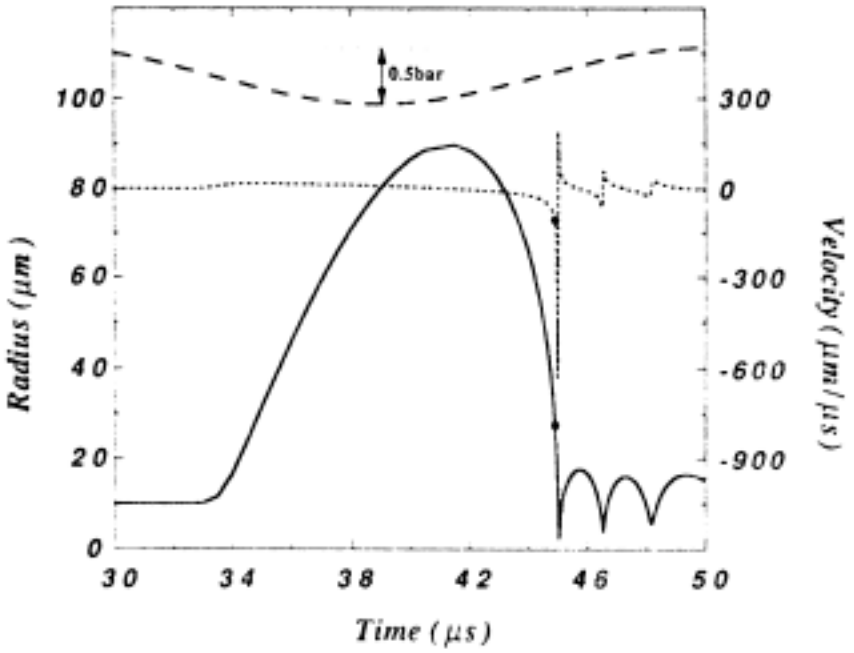

Figure 6. Reprinted from ref. 2, figure 1. Moss's Step 1 calculated history of the bubble interface radius (solid curve) and velocity (short-dashed curve). The long-dashed curve is the oscillatory driving pressure, retarded by the sound transit time into the vicinity of the bubble.

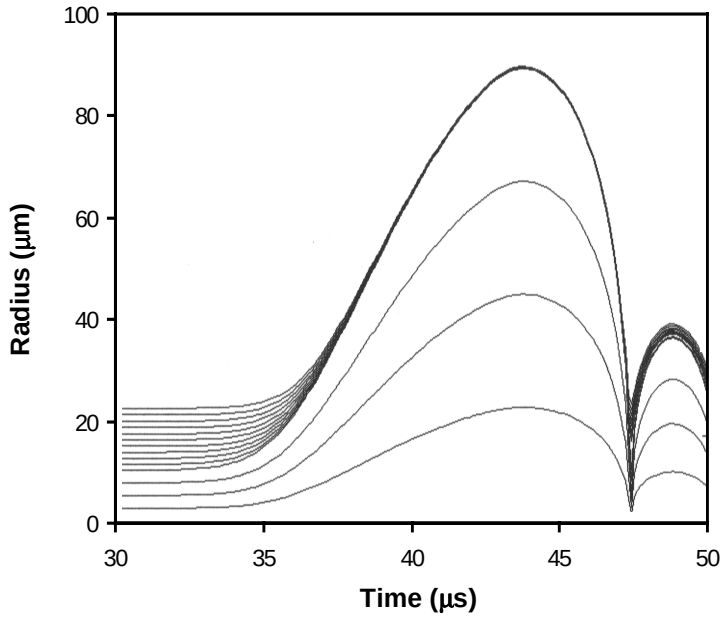

Figure 7. Radius history for the four air zones and the innermost 10 water zones in the first HYADES simulation of the SL test case. Compare this result with that of Moss, et al. in Figure 6. Qualitative and semi-quantitative agreement is readily seen.

III. More Detailed Study of the SL Example

In this section, we'll move to a greater level of detail in our study of the physics and numerics of the bubble simulations. From this work, we've learned a great deal about both the physics involved in sonoluminescence and the techniques required to obtain reliable hydrodynamic simulations in this physical regime.

Calculational and diagnostic techniques

As we performed additional simulations of this SL example, we learned to appreciate the sensitivity of the results to small changes in numerical details of the calculation. This high sensitivity to calculational details is not too surprising, since the behavior of the bubble is clearly a small feature of the overall behavior of the physical system. To illustrate this point: since the radius of the bubble is only 0.001 cm out of 5 cm, the bubble's total volume change between the initial and collapsed stage is only 1 part in $(5000)^3$ or $\sim 1 \times 10^{-11}$ of the total system's volume. Thus, if one looks at the motion of the bulk of the water surround, there is *almost* nothing happening; however, the key to the bubble dynamics is in the "almost" part of that statement. Given the large density ratio between the water surround (1 g/cc) and the air in the bubble (initially 1.31×10^{-3} g/cc), the mass of the bubble is an even smaller fraction of that of the whole system: $\sim 1 \times 10^{-14}$! One can readily imagine, given these ratios, that the bubble's behavior is very dependent on small details of the treatment of the entire system. Expressed in another way, performing a simulation of a bubble's dynamics with even reasonable accuracy is somewhat of a "tour de force" for a hydrodynamics code.

One example that we've encountered emphasizes this high sensitivity to numerical details: changing the simulation timestep controls can sometimes produce substantial changes in the bubble's behavior. Another aspect of the numerics that we have not yet directly investigated is a potentially strong sensitivity to low levels of distortion in the sinusoidal driving pressure waveform.

To minimize generation of these potential spurious numerical events, we adopted a very stringent control of the simulation conditions. For example, we found it beneficial to manually reduce the simulation timestep as the time of final collapse approaches. Since the shift between freely imploding water and the onset of stagnation as the bubble gets denser and hotter occurs very suddenly, the code can approach the collapse with a timestep that is large enough to create a random variation in stagnation time, depending on exactly when the collapse occurs relative to the timesteps of the calculation. In addition, any calculation that appeared anomalous or had any unusual occurrence (a circumstance that arose only once) was repeated, and consistency was required before the analysis was taken seriously.

The apparent results of a calculation can depend on "little" details of the run diagnostics, as well. Consider that the bubble's "dwell-time" near peak compression is $\sim 10^{-11}$ s, whereas the total simulation time is $\sim 10^{-5}$ s. Since a convenient number of points to plot (or number of edits to save) is $\sim 10^3$, one can see that using constant-frequency plotting (or editing) is likely to miss the time of peak compression, perhaps by quite a bit. To minimize this problem, we used a scheme of stepwise logarithmic changes in the plot and edit frequencies: they were decreased in steps of a factor of 4 in a series of time intervals centered on the expected collapse-time of the bubble.

As a result of these effects, we found it convenient to run a first, rough calculation to establish when the bubble collapse occurs under a given set of modeling assumptions. Then, a finely tuned calculation was run, starting from one of the dumps saved in advance of the collapse, in which we adjusted the timestep and edit frequencies to accommodate the individual case being examined.

Although there are possible numerical pitfalls here, two things should be noted. First, we've made a serious attempt through multiple calculations and "sanity testing" to be as sure as possible that we haven't fallen into a numerical pit. Second, not all features of the calculations are equally sensitive to numerical details. Except where noted below, we find the results of a "good" calculation to behave fairly robustly. The numerical difficulties appear to be under adequate control. The calculations presented appear reliable for most of the behavior and physical quantities of interest in this work. We've found that obtaining adequate plot or edit frequencies was more significant in obtaining accurate results than our manual reductions of the timestep. HYADES own timestep controls were adequate to obtain good simulations of the bubble's dynamics in most cases. Still, we obtained somewhat more consistent and robust simulations (avoiding the occasional "timestep crash") when we manually adjusted the maximum timestep to a value of 1% of the plot/edit frequency.

Numerical Accuracy, Speed, and Convergence

A Lagrangian hydrodynamics code divides the matter being simulated into "cells" or "zones" that should be infinitely small, if the finite difference equations being solved are to reproduce the results of the original differential equations describing the hydrodynamics. However, one must always, in practice, make a trade-off between calculational resolution and the simulation run-time. Higher zoning resolution, and therefore, higher numerical accuracy, always (except for very special cases) entails longer run-times. HYADES shows excellent scaling of the run time with the number of zones for this problem, with $t_{run} \sim (N_{zones})^2$. This is essentially equal to the best scaling that can be expected, based on a simple analysis of the physical regime of the simulations.

In a thorough study of a given physical situation, one usually performs a series of calculations with different zoning configurations and increasing zoning resolution. The results are then analyzed in order to (a) determine what distribution of zones leads to the most efficient numerical treatment of the problem, (b) determine a desirable trade-off between simulation accuracy and run-time, and (c) ensure achieving the degree of convergence required for adequate accuracy and reliability of the results.

At the outset of this work, we had a long list of physics and design questions to be answered in a field that was new to us, we were initially limited to current (high-end) PC-computing speeds, and we wished to obtain results on a fairly compressed research timescale and budget. Thus, our starting point has been guided by Moss's previous work and our calculations limited to simulation times that are tolerable. The first HYADES calculation reported here took about 24 hours to run on a 733 MHz Pentium III PC, using zoning somewhat coarser than Moss's "Step-1" calculation [ref. 2, p. 2980]. Results below will illustrate that we have definitely not performed the simulations in a region of strong, guaranteed numerical convergence, even as we allowed the run time to increase to several days. The zoning range we covered is, we believe, sufficient to give an indication

of resolution-related sensitivity and accuracy of the calculations, and to obtain useful simulations of moderate accuracy.

The dominant factor that affects the length of a hydrodynamic bubble simulation is the Courant condition, which places a time-varying upper limit on the timestep (the time advance per cycle). The calculation will be numerically stable if and only if the timestep is less than the time required for a sound wave to cross a zone. For much of the simulation, the timestep-limiting part of the calculation is thus the zone with the highest sound speed and the smallest physical dimension (at a given time). Early in the calculation, this is the water zone at the interface with the gas bubble. In our first successful calculation, with 500 zones in the water, and an innermost water zone size of ~1 μm, the sound speed of 1.5 x 10^5 cm/sec implies a timestep of about 700 ps, initially. However, since we track the bubble through an expansion of a factor of ~9 in radius, and the thickness of the innermost water zone decreases as $1/r^2$ during this expansion, the timestep varies between the initial value and ~7 ps over most of the problem time. Later in the run, when the bubble collapses, things get even worse! At this point, the rapid changes and small gas zones in the collapsing bubble lead to timesteps in the ~1 ps range. We need to follow the bubble's evolution over a total problem time of ~30-50 μs. Thus, a typical simulation of the resolution being used here takes ~1-10 million cycles. With an execution time of ~40 ms/cycle (using ~500 zones on the current PC), one arrives at run times of ~24 hours, for the coarse-zoned case.

Several ways to obtain shorter run times can be considered in a longer-term, higher-budget project. They include algorithm- and coding- optimization, and use of more powerful computer hardware. Moss found, in his later work, that use of implicit hydrodynamics to simulate the early-time bubble motion reduced the required run times enormously, so this is clearly an important avenue to pursue.

Overview and Results of the Zoning Study

Before we present our most reliable and accurate simulation results, we discuss what we've learned about optimizing the zoning setup, and what can be said about numerical reliability and accuracy from the zoning study. For the purposes of determining what zoning distribution leads to highest accuracy at lowest cost, we divided the problem into four regions, according to expected functional distinctions. Figure 8 shows the four regions chosen. We considered the gas as a single region. Since we were most concerned with the effects of the large mass-mismatch between the innermost water zone and the outermost gas zone, we divided the water into three regions: "Pusher-1," "Pusher-2," and "Surround." To make the functional distinction, we started from the initial zoning in the water region, which used 500 zones, with each successive zone larger in Δr by a factor of 1.0127. We somewhat arbitrarily chose the first water zone (initially, Δr = 1.14 μm) as Pusher-1, and the second water zone as Pusher-2. As we vary the zoning in these two regions, we maintain their physical boundaries at constant (initial) positions in the water. We expect some fraction of the total mass of these two pusher regions to participate intimately in determining the configuration of the gas near stagnation. For zones further out in the water, we expect gradients to be less significant, and we also anticipate that the coupling of the energy of these zones into the bubble dynamics will be less efficient. Thus, we treat the remainder of the water zones as the

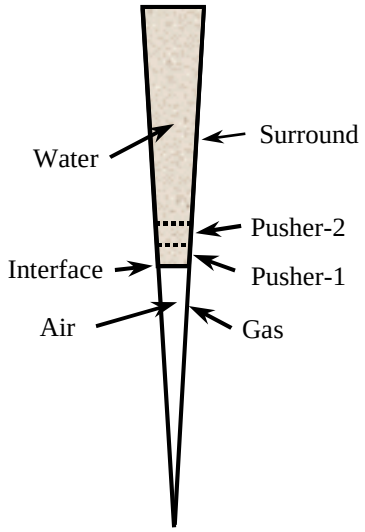

Figure 8. Schematic diagram of the physical regions considered for the zoning and convergence study. Drawing is a pie-diagram representation of a segment of the sphere, and is not to scale.

"Surround." We made one other simplification to reduce the number of zoning regions to three: we decided that the number of zones in the two pusher regions would be kept equal, i.e., if we double the zoning in Pusher-1, we also double the zoning in Pusher-2. This should allow the hydrodynamics enough freedom to resolve without zoning bias the extent to which the two pusher regions' kinetic energy will participate in the compression of the gas.

Having identified three regions of particular interest, we are now equipped to vary the zoning in each to determine what changes occur in the simulation. Figure 9 shows a schematic map of the 3-dimensional parameter space for the zoning study. We varied the number of zones in each region by steps of a factor of two each. Thus, we varied the gas zoning from 4 to 32 zones, the pusher-1 (and pusher-2) zoning from 1 to 8 zones, and the surround zoning from 500 to 1000 zones. This allowed us to explore a factor of 8 range in the gas and pusher zonings, and a factor of 2 in the surround zoning.[15]

First, as we had suspected, the zoning study shows that we are not able to reach fine enough zoning to demonstrate a fully converged, high-accuracy calculation of the bubble dynamics. We found a qualitative shift in the simulations as the zoning was refined. The coarse-zoned runs compressed the bubble nearly adiabatically (Fig. 10a), while the finest-zoned runs drove a significant shock through the gas late in the compression phase (Fig. 10b). This shock is nearly invisible in the coarsest-zoned runs, and becomes stronger and more obvious as the mesh is refined. Over the available range of zone sizes, it is hard to be sure that we have seen the fully converged shock behavior.

Some of the calculated quantities appear to be fairly robust and predictable, i.e., they vary smoothly as the zoning is refined, and don't depend strongly on the strength of the shock during compression. An example of this smooth behavior is shown by the peak

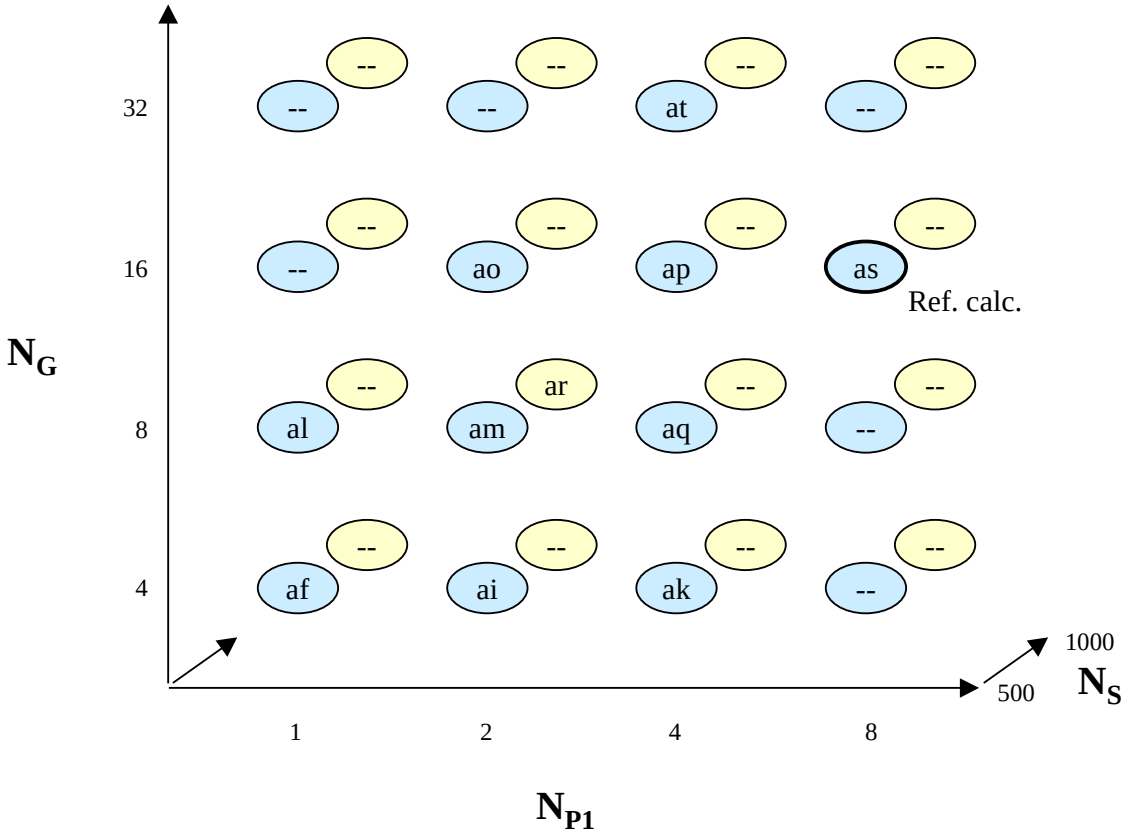

Figure 9. Schematic map of the mesh distributions run in the zoning and convergence study. See text for discussion.

density of the gas zone nearest the interface, plotted in Figure 11. Although the range of variation is significant, the variation is nearly linear and one could have reasonable confidence in the degree of convergence, especially in the finest meshes. Other quantities show substantial, non-linear changes as the mesh becomes finer. A good example of this is the density of the central zone in the calculation, plotted in Figure 12. Here, the effect of the shock during compression is quite noticeable, and the surface is sufficiently nonlinear that it is difficult to ensure full convergence, even using the finest accessible meshes. Good convergence appears possible, but it is not assured.

By comparing the behavior of the central density and the central temperature, we can address the issue of whether significant, anomalous wall heating is occurring in this calculation. Figure 13 shows the central temperature's behavior. The central zone reaches a much higher temperature in the finest-zoned runs. However, the density does not exhibit a correspondingly large decrease. Thus, we believe that anomalous wall heating is not occurring to a significant degree in the most important simulation regime for this case.

We find the results of the zoning study to be encouraging, even though we haven't reached the ideal of guaranteed convergence. The results of the finest-zoned calculations appear to be accurate enough for our purposes in roughly scoping the behavior of SL and

a)

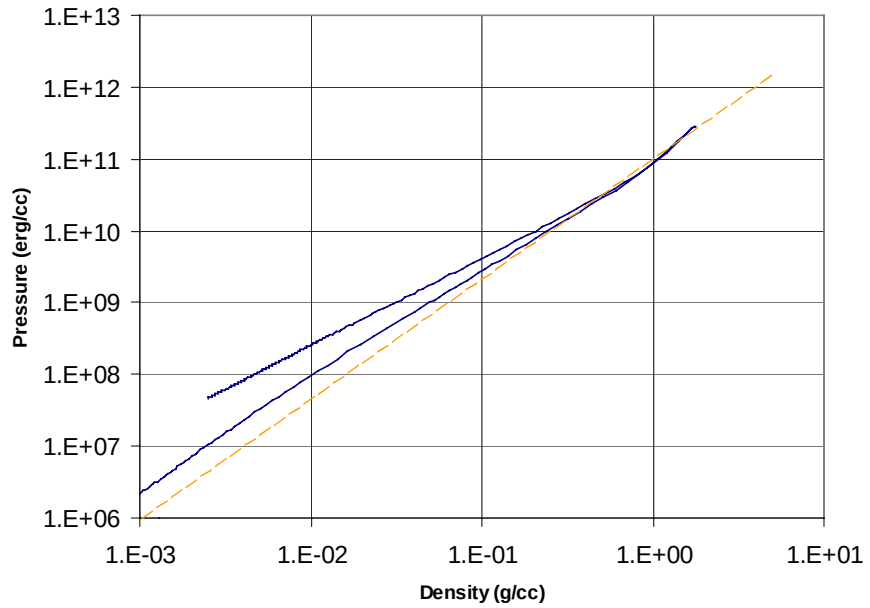

b)

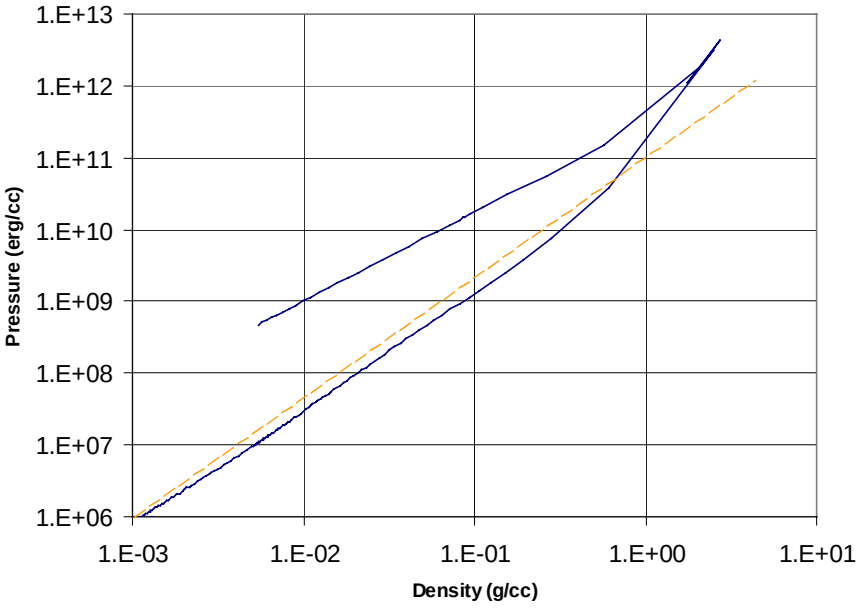

Figure 10. Isentropes calculated for the central zone in the HYADES simulation of the bubble dynamics. (a) is for a calculation that used 4 gas zones, 1 zone in each pusher region, and 500 zones in the surround. (b) is the result for a calculation that used 16 gas zones, 8 zones in each pusher region, and 500 zones in the surround. Note that the higher resolution calculation shows a fairly strong shock reaching the center near the end of the bubble collapse. The light dashed lines are the isentrope for a $\gamma = 5/3$ ideal gas under adiabatic compression, shown for reference.

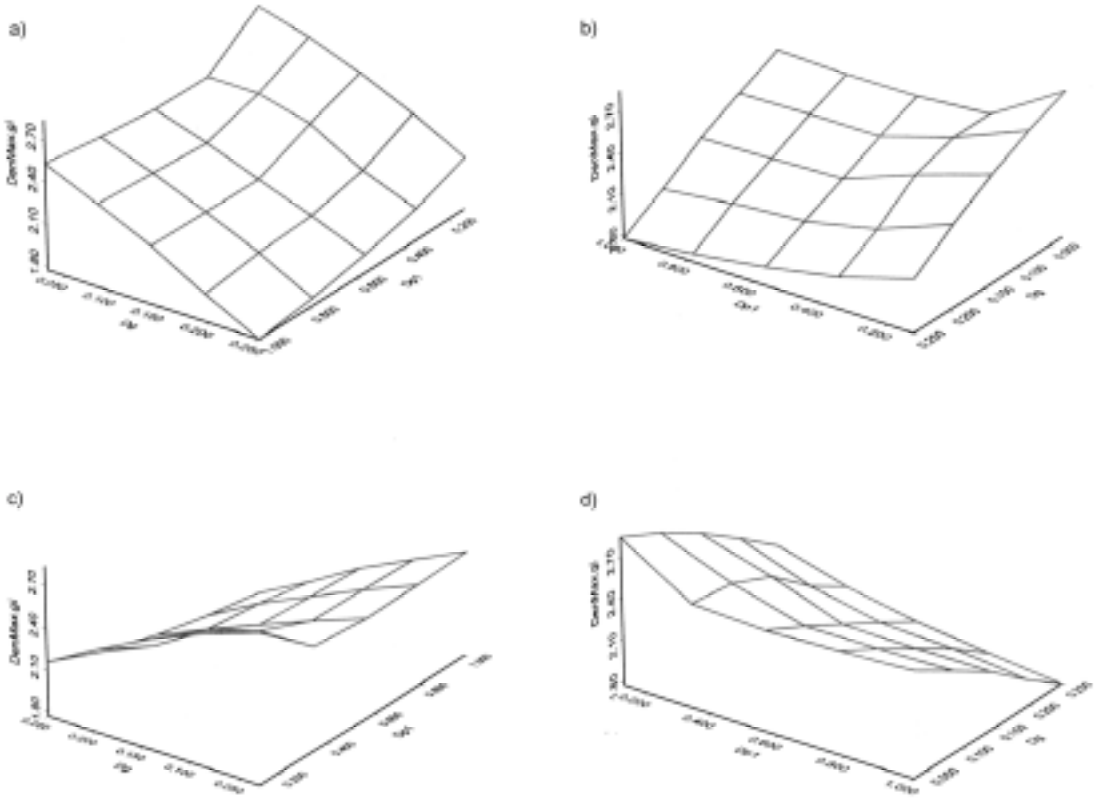

Figure 11. Maximum HYADES-calculated gas density attained near the bubble interface as a function of the initial (relative) zone sizes in the gas and pusher-1 regions. Four views have different viewing angles, namely (a) 35°, (b) 125°, (c) 215°, and (d) 305°. The peak gas density achieved near the outside of the bubble varies relatively slowly and smoothly as the mesh is refined, indicating fairly predictable convergence.

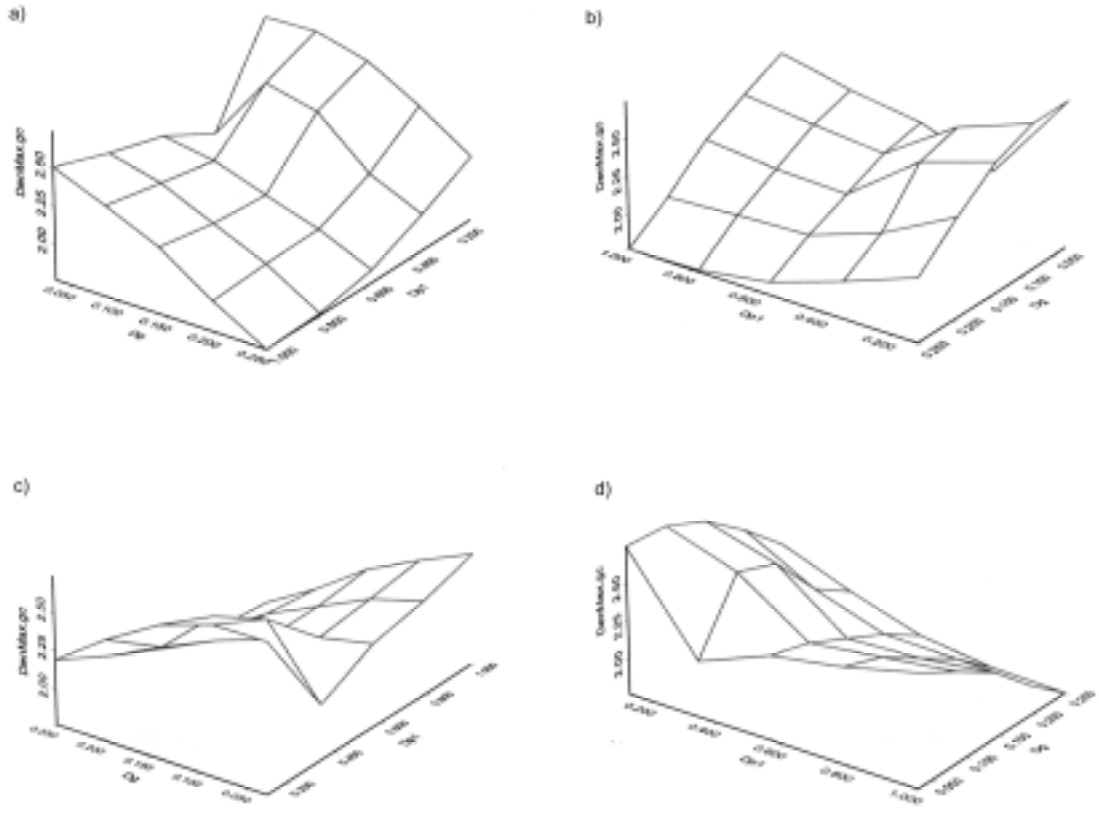

Figure 12. Maximum gas density at the center of the bubble behaves much more non-linearly as the mesh is refined. One significant factor in this behavior is the development of a strong shock in the finer-zoned runs, as shown in Fig. 10. Even in this case, as the mesh is refined, the convergence appears to be approaching a linear regime.

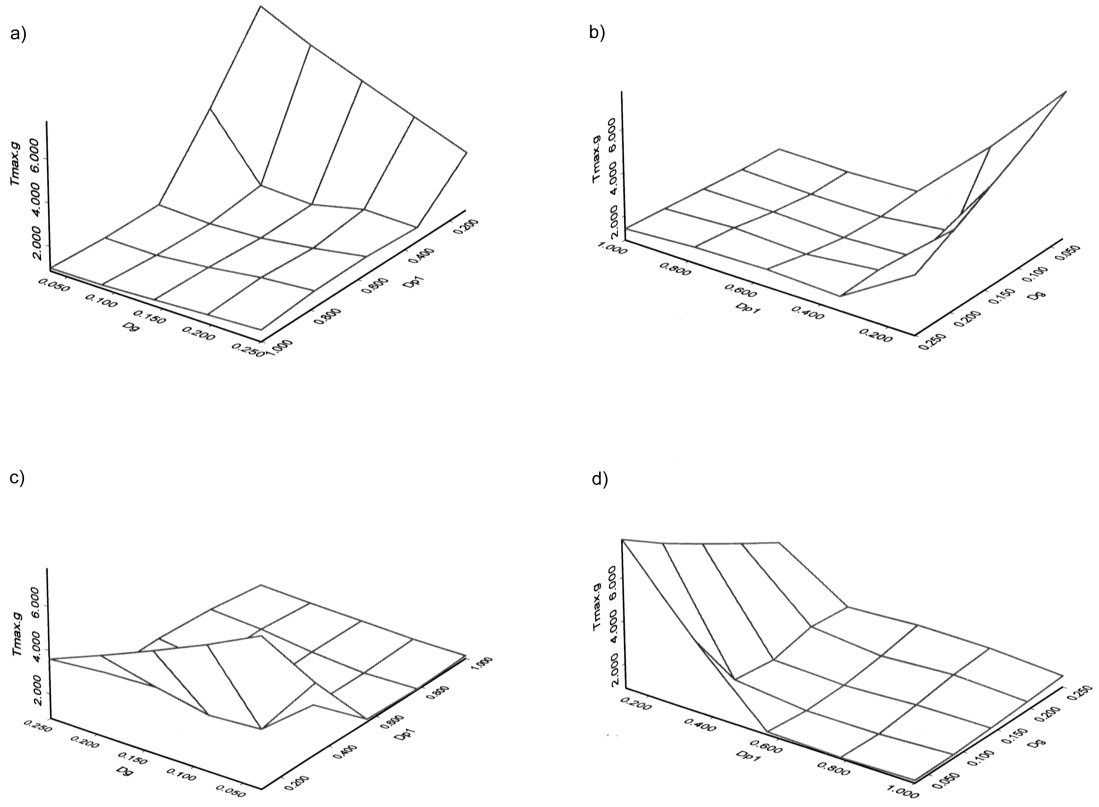

Figure 13. Maximum gas temperature as a function of initial zone sizes in the gas and pusher-1 regions. The formation of the shock in finer-zoned calculations makes a very strong, non-linear change in the central temperature. The temperature is still increasing rapidly with decreasing zone-size, even for our finest-zoned runs. Comparing the shape of this surface with that of Fig. 12 offers strong evidence that the anomalous wall heating seen in the Noh test problem is not occurring significantly in the SL calculations.

SF bubbles. In our final analysis, we will assign rough "uncertainties" to the calculated quantities, based on our convergence tests. This, of course, does not compensate or treat systematic errors in the code/physics. To address the overall reasonableness of the results, we will compare our calculations' features with Moss's simulations and with experimental data.

Stagnation processes and conditions: "Reference" calculation

In this section, we show the events and conditions HYADES predicts near the bubble's peak compression. We present here a bubble calculation that is identical with the first (Figure 7), except that (1) we have manually adjusted the timestep and the edit frequencies to ensure accurate calculation and monitoring of the final stages of the collapse and (2) we present one of our best calculations to date, i.e., a calculation in which we have increased the number of zones in the gas to 16 and the number of zones in each pusher region to 8 (still 500 zones in the surround). This calculation will be referred to as our "reference" calculation in the remainder of this report.

Figure 14 shows the history of the bubble's collapse phase on an expanded timescale, the 5 ns surrounding the maximum compression. We shall refer to various features of the calculated collapse as we compare our results with Moss, et al., and with experiment in the next two sections.

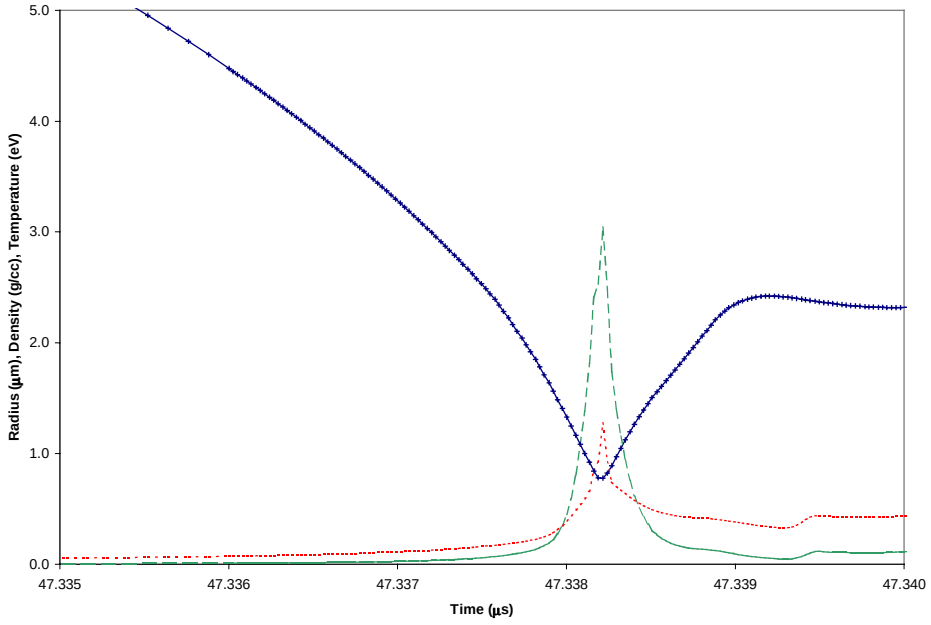

Figure 14. Bubble radius (solid line with dots at the plotting times), and typical bubble density (long-dashed line) and temperature (short-dashed line) histories near the bubble's collapse time. In this calculation, without thermal conduction effects, the peak temperature and pressure occur near-simultaneously with the peak gas density and minimum bubble radius. The density history shown here is used to estimate the duration of the radiation pulse emitted upon bubble collapse.

Comparison of "Reference" HYADES Calculation with Moss, et al.

Table 1 compares the results we obtain using HYADES with those reported by Moss, et al. In maximum bubble radius, maximum inward interface speed, collapse time, minimum interface radius, and maximum density, our results are in good agreement with those of Moss, et al.

	Moss, Ref. 2 (Step 1)	Moss, Ref. 2 (Step 2)	HYADES (Reference calc.)	This work ("Best value," zoning study)	This work ("Uncertainty," zoning study)
R_{max} (μm)	90.	--	90.	90.	3.
u_{max} (cm/μs)	0.065	0.31	0.31	0.36	0.08
$t_{collapse}$ (μs)	45.1	45.04	47.3	47.0	0.6
R_{min} (μm)	2.4	0.64	0.78	0.72	0.1
D_{max} (g/cc)	--	3. - 9.	2.8	2.8	0.8
T_{max} (eV)	--	15.-140.	7.0	8.	2.
P_{max} (Mbar)	--	20. - 225.	4.3	6.	2.
$\Delta t_{emission}$ (ps)	--	[< 10.]	[70.]	[50.]	[20.]

Table 1. Comparisons of the results reported by Moss, et al.[2] with the results of this work. R_{max} is the bubble radius at the time of maximum expansion; u_{max} is the maximum inward speed of the interface; $t_{collapse}$ is the time of minimum bubble radius, R_{min}; D_{max}, T_{max}, and P_{max} are the corresponding maximum gas density, temperature, and pressure at stagnation; $\Delta t_{emission}$ is the estimated FWHM of the photoemission pulse. Our results agree well with those of Moss, et al. in the first five of these quantities. Our calculated peak temperature and pressure are lower than Moss's, probably due to coarser gas zoning. We expect other physics, not included here (or in ref. 2), to further reduce the central temperature.

Our results differ significantly, however, in the calculated maximum temperature and pressure. Also, although our emission times are estimated using a simple analytic model, we estimate a significantly longer emission time than Moss, et al. calculated using their radiation model. All these disagreements are "consistent," in the sense that they can all be considered as probable results of Moss's much finer zoning in the gas region, which allows his calculations to follow spherical convergence to a greater degree. Where one ceases to trust the 1-D, hydrodynamics-only modeling is a matter for future work. Our expectation at this point is that the physics processes omitted from the modeling at this stage (e.g., thermal conduction, better ionization and radiation physics, asymmetries, fluid instabilities) are likely to reduce the peak temperatures from those we quote as our "best" values, rendering the question of what happens at higher zoning resolution somewhat moot.

Comparisons with SL Experiments and Measurements

What can be said about our calculational results on the basis of measurements to date? Clearly, comparisons with experiment at this point must be somewhat tentative and broad, since the quality of the current modeling is limited by (1) physics exclusions, (2) omitting calculational steps needed to match the calculated quantities to the (somewhat different) quantities that can be measured in experiments to date, and (3) incomplete numerical convergence. Nonetheless, we believe the following comparisons lend some overall credibility to the relevance of our calculations.

Both time-dependent and minimum bubble size are extremely difficult to measure. Just as the small spatial scales and short timescales pose a calculational challenge, so do they limit the accuracy and range of measurements. The technique leading to the most direct and accurate results in measuring the bubble dynamics is Mie scattering. Using this technique, Lentz, et al.[16] were able to measure a bubble's radius over a significant part of the collapse, and they obtained reasonably good correspondence between their measurements and the interface trajectory calculated by Moss, et al.,[2] down to a minimum observable bubble radius of about 7 μm. The minimum bubble radius is therefore not well measured, and we can only claim reasonable agreement between calculations and measurements for the early part of the collapse trajectory. Our results are in close enough agreement with Moss's that we obtain similarly satisfactory agreement with the measurements.

A number of researchers[17-20] have measured the light emission spectra for various cases of single-bubble (SBSL) and multi-bubble (MBSL). Hiller, et al.[17] reported good fits to the measured SBSL spectrum using blackbody spectra of 25000 K to 50000 K (~2-4 eV), depending on the operating temperature of the SL bath. More recently, measurements[20] of the time-dependence of the emission as a function of wavelength show pulse durations of 35 to 110 ps for various partial pressures of air in water. Hiller's measurements[20] include time-resolved data suggesting the emission pulse width is fairly constant over the spectral range of 200 – 800 nm. This is interesting data, and with some additional work, we would be able to compare the HYADES simulations with these features.

The temperatures obtained in our calculations appear adequate to produce a spectrum of the nature observed. In order to estimate the emission pulse durations that might be produced from the conditions calculated, we note that the emission timescale would be dominated by the density-dependence of the emission, since, for both bremsstrahlung and free-bound radiation, the radiated power has the approximate scaling-dependence $P_{rad} \sim \rho^{2}$. The temperature dependence is somewhat weaker, e.g., $T^{1/2}$ for bremsstrahlung, so the effect of the temperature variation with time is less than that of the density. Based on this, we estimated an emission pulse FWHM of about 20 – 70 ps for the calculated example (still quite uncertain due to incomplete numerical convergence), which is generally reasonable compared with the measured pulse durations.

In passing, we note that some experimental work on SL has addressed issues of overall bubble shape-stability.[21] At this early stage of our work, we are not able to comment on this subject, except to note that, on theoretical grounds, the issues of bubble stability and symmetry cover a wide range of rich and subtle physical processes.

At the present crude level of comparison, it is too early to point to anomalies between the calculation and experiments, or to claim agreement. The only preliminary conclusion we wish to draw from this crude comparison with experiment is that we find order-of-magnitude indication that the calculations are not in contradiction to experimental information. In order to proceed to the next level of comparison accuracy, the modeling needs to be extended to include more of the omitted physics, to calculate quantities such as the x-ray emission spectrum and its time dependence in a more detailed way, and to reach more definitive levels of numerical convergence.

IV. Summary and Conclusions

We have calculated the dynamics for a prototypical case of sonoluminescent bubble collapse using the HYADES Lagrangian hydrodynamics code. A series of hydrodynamic test problems has been performed to become familiar with HYADES' performance in a variety of hydrodynamic situations where analytic solutions are known, with generally favorable results. Only the Noh problem revealed circumstances in which HYADES' hydrodynamics generates significantly anomalous results; the signature of the "wall heating" anomaly has been used to verify that this anomaly does not arise at a significant level in the SL bubble simulations performed to date.

To date, the predictions and behavior of only the simplest HYADES modeling have been explored in detail. Most of this work employed a physical model that includes only 1-D spherical hydrodynamics using a tabular Equation of State. Much additional work is needed to examine the effects of mass diffusion, ionization, thermal conduction, radiation, asymmetries, and fluid instabilities.

We performed a zoning study to optimize the distribution of zones and to determine the extent to which our calculations can approach numerical convergence with current (high-end PC) computer resources. Although we have not reached mesh sizes that guarantee full convergence, the zoning study allowed us to estimate "best values" and rough "uncertainties" for the various calculated quantities.

The physical conditions predicted by our best HYADES calculations to date and by taking the infinite-resolution limit of the zoning study results have been compared with the published results of Moss, et al. We find good agreement with their work in the minimum interface radius (0.7 μm), the maximum bubble radius (90 μm), the maximum interface velocity (0.36 cm/μs), and the maximum gas density reached (2.8 g/cc). Our calculations reach lower peak temperatures and pressures than those reported by Moss, et al., which can be understood in terms of our lower calculational resolution. Calculational resolution is not the only issue here, however. There are a number of physical effects that neither set of calculations took into account that would lower the peak stagnation temperature.

Using simple estimates, we compared the results of our simulations with the results of measurements of the bubble radius history, and the x-ray spectrum and time dependence. At the current level of comparison, the correspondence between our calculations and the measurements is generally reasonable.

This work has achieved a broadly satisfactory starting point. We are fairly confident that the techniques and tools developed and tested in this work are adequate to begin useful exploration of the behavior and performance of various Sonically Driven

Fusion (SF) reactor scenarios. We hope to be able to answer some qualitative and semi-quantitative questions regarding SF better than has been possible to date, and to be able to guide SF reactor design and testing well enough to enable achievement of a detectable level of fusion yield, in the not-too-distant future.

We find through order-of-magnitude comparison with experiments to date that the calculations do not disagree with measurements at this level, providing some encouragement that the modeling is relevant to experimental conditions. We hope future work with better calculations and measurements under well-characterized conditions will allow us to assess the modeling's relevance and accuracy at a more demanding level. Improvements both in the accuracy of "single-point comparisons" and in "scaling studies" over wider parameter ranges should enhance our predictive confidence.

Work is underway to obtain improved code capabilities at reduced computing costs. We anticipate being able to do improved simulations as this work continues.

Acknowledgements

This work was funded by Impulse Devices, Inc. The author thanks Ross Tessien, President, and Felipe Gaitan, Chief Scientist, for support and helpful discussions throughout this work.

The author thanks Damon V. Giovanielli, Roger D. Jones, Albert G. Petschek, and Richard R. Silbar for stimulating discussions as the work proceeded. Thanks are due, as well, to Jon T. Larsen for his generous support in the use of HYADES throughout this work, and to Sven G. Redsun and R. D. Jones for their initial efforts toward developing a new hydrocode that we hope will improve our SL/SF modeling capabilities in future work. Finally, the author thanks Jacques Delettrez, Glenn R. Magelssen, William C. Moss, and George B. Zimmerman for helpful comments on a draft of this report.

References and Notes

[1] "Sonoluminescence and Bubble Dynamics for a Single, Stable Cavitation Bubble," D. F. Gaitan, L. A. Crum, C. C. Church, and R. A. Roy, *J. Acoust. Soc. Amer*. **91**, 3166 (1992).

[2] "Hydrodynamic Simulations of Bubble Collapse and Picosecond Sonoluminescence," W. C. Moss, D. B. Clarke, J. W. White, and D. A. Young, *Phys. Fluids* **6**, 2979 (1994).

[3] "HYADES Users' Guide," J. T. Larsen, Cascade Applied Sciences, Inc., Document CAS061 (Version PP.05.13, October, 1999).

[4] "HYADES- A Plasma Hydrodynamics Code for Dense Plasma Studies," J. T. Larsen and S. M. Lane, *JQSRT* **51**, 179 (1994).

[5] "Calculated Pulse Widths and Spectra of a Single Sonoluminescing Bubble," W. C. Moss, D. B. Clarke, and D. A. Young, *Science* **276**, 1398 (1997).

[6] "Computed Optical Emissions from a Sonoluminescing Bubble," W. C. Moss, D. A. Young, J. A. Harte, J. L. Levatin, B. F. Rozsnyai, G. B. Zimmerman, and I. H. Zimmerman, *Phys. Rev. E* **59**, 2986 (1999).

[7] "SESAME: the Los Alamos National Laboratory Equation of State Database," S. P. Lyon and J. D. Johnson, Los Alamos National Laboratory Rpt. No. LA-UR-92-3407 (1992).

[8] National Bureau of Standards (1997); data provided by J. T. Larsen as a component in the HYADES Pro code package (Jan., 2000).

[9] The SESAME EOS tables we had available for water (#7155 was the most recent) were tried and found to be unsatisfactory in the physical regime of SL. It is important in the SL application for the water EOS to support negative pressures (tension), a feature that is suppressed in the SESAME EOS. The numerical effects of "clipping" the water pressure at 0 are disastrous to simulations in SL cases where spherical convergence makes the time-varying pressure in the water exceed the ambient pressure of ~1 bar. We note that the behavior of water under tension has been studied for 150 years, and negative pressures can exceed –1000 bars without cavitation, under controlled conditions. Of course, the tensions obtained in SL calculations are much less than that level. A summary of the status of negative pressures in water is given in the article "Negative Pressures and Cavitation in Liquid Helium," H. Maris and S. Balibar, *Phys. Today* **53** No. 2, 29 (Feb., 2000).

[10] The Courant time step condition is sometimes applied with a "safety factor." This can be important in multidimensional calculations. In this work, the user multiplier on the Courant condition was set to the HYADES default value of 1.0. No signs of numerical hydrodynamic instability were observed.

[11] "Infinite Reflected Shock Test Problems in Spherical Geometry," W. F. Noh, Lawrence Livermore National Laboratory Internal Memorandum (May 25, 1982).

[12] "Lie Group Invariance Properties of Radiation Hydrodynamics Equations and their Associated Similarity Solutions," S. V. Coggeshall and R. A. Axford, *Phys. Fluids* **29**, 2398 (1986).

[13] Ya. B. Zel'dovich and Yu. P. Raizer, **Physics of Shock Waves and High-Temperature Hydrodynamic Phenomena** (Academic Press, New York, 1967).

[14] The choice of 0.15 C was motivated by two considerations. First, with the hydrodynamic modeling used here, the initial temperature of the bubble matters only to the extent that it determines the gas density for the initial equilibrium pressure, and it only matters as an absolute temperature. Thus, 0.15 C, or 273.3 K is only about 5% different from room temperature of ~15 C, or 288 K. The bubble dynamics are thought to be insensitive to this

modest change in initial conditions. Second, some SL experiments have been done using cooled baths, just above freezing. Under these circumstances, the SL is more intense, and this is believed by some to be caused by water's lower vapor pressure near its freezing point. Since we are using dry air in the gas bubble, we chose the temperature that corresponded most closely with that assumption. When time permits, it might be interesting to perform another HYADES calculation at 15 C, to verify that the effects of a 5% change in initial temperature and density are small, at least for the physical model used here.

[15] It is perhaps worth noting that, if we had tried to achieve the same factor of ~8 dynamic range in zoning by varying the zoning in all three regions of the problem simultaneously, the finest-zoned run would increase by a factor of about $(8)^2$, leading to a run time of more than 60 days. That's not completely infeasible, but that approach would be significantly more costly than the study we've carried out here, and it would also provide less information about where the resolution is needed and where it is redundant.

[16] "Mie Scattering from a Sonoluminescing Bubble in Water," W. J. Lentz, A. A. Atchley, and D. F. Gaitan, *Appl . Optics* **34**, 2648 (1995).

[17] "Spectrum of Synchronous Picosecond Sonoluminescence," R. Hiller, S. J. Putterman, and B. P. Barber, *Phys. Rev. Lett.* **69**, 1182 (1992).

[18] "Comparison of Multibubble and Single-Bubble Sonoluminescence Spectra," T. J. Matula, R. A. Roy, and K. S. Suslick, *Phys. Rev. Lett.* **75**, 2602 (1995).

[19] "Spectra of Single-Bubble Sonoluminescence in Water and Glycerin-Water Mixtures," D. F. Gaitan, A. A. Atchley, S. D. Lewia, J. T. Carlson, and X. K. Maruyama, *Phys. Rev. E* **54**, 525 (1996).

[20] "Time-Resolved Spectra of Sonoluminescence," R. A. Hiller, S. J. Putterman, and K. R. Weninger, *Phys. Rev. Lett.* **80**, 1090 (1998).

[21] "Observation of Stability Boundaries in the Parameter Space of Single Bubble Sonoluminescence," R. G. Holt and D. F. Gaitan, *Phys. Rev. Lett.* **77**, 3791 (1996).

[22] "Experimental Observations of Bubble Response and Light Intensity Near the Threshold for Single Bubble Sonoluminescence in an Air-Water System," D. F. Gaitan and R. G. Holt, *Phys. Rev. E* **59**, 5495 (1999).

NOTICE

This report was prepared as an account of research performed by Adaptive Network Solutions Research, Inc. (ANSR, Inc.) and consultants of Impulse Devices, Inc. (IDI), and sponsored by Impulse Devices, Inc. Neither IDI, nor ANSR, Inc., nor any of the authors makes any warranty, express or implied, or assumes any legal liability or responsibility for the accuracy, completeness, or usefulness of any information, apparatus, product or process disclosed.